International Journal of Innovative Computing, Information and Control
Volume **19**, Number **5**, October **2023**

ICIC International ©2023 ISSN 1349-4198
pp. **1455–1470**

SLIDING MODE OBSERVER-BASED SENSOR FAULT DIAGNOSIS FOR LITHIUM-ION BATTERY PACKS

Dezhi Xu[1], Yunchen Ma[1], Weilin Yang[1,*], Tinglong Pan[1] and Zhenlan Dou[2]

[1]School of Internet of Things Engineering
Jiangnan University
No. 1800, Lihu Avenue, Wuxi 214122, P. R. China
{ xudezhi; tlpan }@jiangnan.edu.cn; 6201920003@stu.jiangnan.edu.cn
*Corresponding author: wlyang@jiangnan.edu.cn

[2]State Grid Shanghai Municipal Electric Power Company
No. 677, Jumen Road, Huangpu District
Shanghai (World Expo National Network Pavilion) 200023, P. R. China
douzhl@126.com

Received January 2023; revised April 2023

Abstract. *Battery management system (BMS) is a significant element of battery energy storage system, which serves the data collection, state estimation and fault diagnosis functions. The real-time diagnosis of sensor fault is the key to ensuring the safe and reliable operation of the battery system. This paper presents a model-based sensor fault diagnosis scheme. The mathematical model of the battery is established based on the Thevenin equivalent circuit. A sliding mode observer (SMO) is used to estimate the terminal voltage and state of charge (SOC) of the battery pack. The output voltage estimation is used to make comparisons with the measured value and generate residual. The residual error is evaluated by a statistical reasoning method, cumulative sum (CUSUM), to determine whether the fault exists. The effectiveness of the proposed sensor fault diagnosis scheme is verified by simulation under the dynamic stress test (DST).*
Keywords: Lithium-ion battery pack, SOC estimation, Sensor fault diagnosis, Sliding mode observer, Cumulative sum

1. **Introduction.** With the rapid development of new energy industry, energy storage system, as an integral part of new energy electric vehicle and energy storage grid, plays an important role of energy storage and peak shaving. Lithium-ion batteries are widely used in energy storage system for high energy density and less pollution [1,2]. The lithium-ion battery system mainly includes battery cells, battery management system (BMS) and connecting components [3-5]. In the actual operation process, all of the battery cells, BMS and connecting components will experience various types of failures [6]. The BMS is essential to ensure the safety and reliability of the battery pack. Ordinarily, a BMS should be capable of collecting data, estimating state, managing charge or discharge states and detecting faults in the battery system. The implement of these functions relies heavily on the acquisition of current, voltage and temperature data [7]. A battery system is equipped with massive sensors to monitor the current, voltage and temperature of a single cell. Sensor fault will directly result in BMS dysfunction, which will bring about great security hidden trouble [8]. If a voltage sensor fails, the actual battery voltage may exceed the range of nominal charging cut-off voltage and discharging cut-off voltage, which may lead to overcharge and over-discharge. Overcharging and over-discharging have adverse effects

DOI: 10.24507/ijicic.19.05.1455

on the battery capacity; the worst case may lead to internal short circuit fault and thermal runaway [9,10]. If the current sensor fails, it will lead to incorrect estimation of state of charge (SOC) by BMS, thus misleading the power output management of the battery system [11]. Therefore, fault diagnosis of sensor is critical to ensure the safe operation of the battery system.

Data-driven and model-based fault diagnosis technology has been widely used in industrial applications. Data-driven methods aim to use historical data, combine machine learning, information fusion, statistics and other algorithms to achieve fault detection. In [12], with polarization resistance, polarization capacitance and ohmic internal resistance as characteristics, the Grubbs criterion is used to calculate the local abnormal factor to detect the faulty battery. In [13], multi-fault diagnosis is realized based on the improved sample entropy, with a coefficient introduced to the model, the type and the occurrence time of the fault can be assessed, and the sliding window is used to maintain the detection sensitivity and reduce the amount of calculation. However, the difficult point of data-driven methods is to determine the effective fault characteristics. The data-driven method needs the statistical distribution of the historical fault characteristic data of battery operation to realize fault diagnosis. Compared with the data-driven method, the model-based fault diagnosis method can not only analyze the state of the system from the output signal, but also analyze the system fault state from the key state parameters inside the system through state observation. Model-based fault diagnosis methods realize fault diagnosis by comparing residual and threshold values on the basis of defining the mathematical model of the system and system identification [14]. In [15], the adaptive extended Kalman filter (AEKF) is utilized to make estimations of the battery state, and residuals are generated by making comparisons of the estimated value and the measured value. In [16], the estimated SOC is obtained by using recursive least square method and unscented Kalman filter, and compared with the real SOC to detect and isolate the faulty current or voltage sensor. In [17], a thermal diagnosis method for cylindrical lithium-ion battery based on Lyapunov observer is proposed. In [18], the particle filter is used to estimate the temperature and voltage of the battery pack, and the residual error is studied based on the sliding window to detect and isolate the fault of voltage, current, temperature sensor and battery. In [19], a distributed fault estimation observer is designed to make estimations of sensor fault.

Sliding mode observer (SMO) has been previously used for fault detection. When the system works normally, SMO works on the sliding surface with sliding residuals maintaining zero mean value; when a fault occurs, the sliding mode is destroyed. The fault can be detected by comparing its residuals and thresholds. SMO can also reconstruct the fault [20-24]. In [25], a model-based diagnostic scheme is presented that uses SMOs designed based on the electrical and thermal dynamics of the battery. In [26], the sparse data observer is used to diagnose and predict short circuit and open circuit faults.

Motivated by the aforementioned discussions, to enhance robustness and reduce the impact of parameter uncertainty, this paper takes the equivalent circuit based on the least squares identification as the model, the SMO is designed to observe the battery system to enhance robustness. When a fault occurs, the estimated value of the observer produces a residual with the normal value, and the design threshold is compared with the residual. Because of low sensitivity to noise of the sliding mode observer the probability of false alarm of the fault is reduced, and higher accuracy of fault diagnosis can be guaranteed. The main contributions can be summarized as follows.

1) This paper develops a model-based fault diagnosis strategy using SMO. The requirement for accuracy of the battery model is not high, only voltage data and current data

need to be collected, diagnosis results are hardly affected by the measurement noise. The strategy effectively reduces the rate of misdiagnosis of the battery pack.

2) Compared with previous strategies, the proposed strategy can use residuals instead of measurement signals for fault analysis and easily select the threshold value, reduce the impact of unknown interference.

The remainder of this research is organized as follows. Battery modeling is introduced in Section 2. The diagnosis scheme based on SMO and cumulative sum (CUSUM) is presented in Section 3. The battery experimental design, sensor fault diagnosis results and analysis are given in Section 4. The conclusions are shown in Section 5.

2. **Mathematical Model for Battery.** In order to realize model-based fault diagnosis, a clear mathematical model of the battery system is required to capture the electrochemical characteristics. Scholars have proposed many different types of battery models, among which electrochemical models and equivalent circuit models (ECMs) are the most popular methods. However, it is a complicated process to describe electrochemical model behavior owing to its multitudinous partial differential equations. ECMs are widely used in control-oriented applications, for instance, parameter identification, state estimation and fault diagnosis. In order to reduce the amount of calculation and maintain the modeling accuracy, this paper uses Thevenin equivalent circuit to describe each cell in the battery pack. The Thevenin model, as is shown in Figure 1, consists of a voltage source V_{oc}, an ohmic resistor R_{t}, a polarization capacitance C_{p} and a polarization resistance R_{p}. According to Kirchhoff's law, the electrical dynamics of the battery cell can be written as

$$V_{\mathrm{t}} = V_{\mathrm{oc}} + IR_{\mathrm{t}} + V_{\mathrm{p}} \tag{1}$$

$$\dot{V}_{\mathrm{p}} = -\frac{1}{R_{\mathrm{p}}C_{\mathrm{p}}}V_{\mathrm{p}} + \frac{I}{C_{\mathrm{p}}} \tag{2}$$

where I is the input current, V_{p} is the polarization voltage of polarization capacitor C_{p}, V_{t} is the terminal voltage, and V_{oc} is the open circuit voltage (OCV).

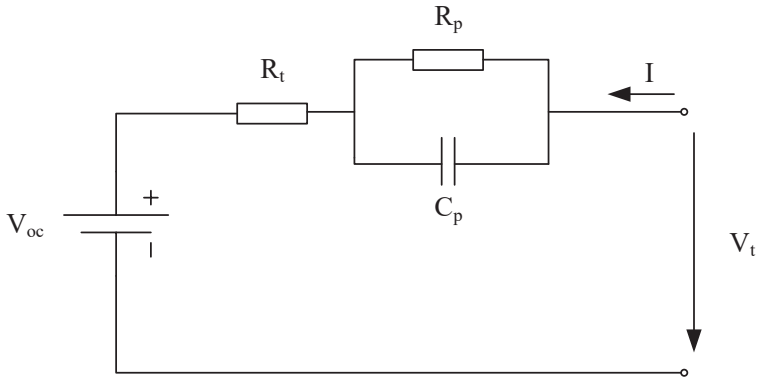

FIGURE 1. Thevenin model

The derivative of SOC can be expressed by usual definition as

$$\dot{Z} = \frac{I}{C_{\mathrm{n}}} = \frac{1}{R_{\mathrm{t}}C_{\mathrm{n}}}\left(V_{\mathrm{t}} - V_{\mathrm{oc}} - V_{\mathrm{p}}\right) \tag{3}$$

The battery OCV can be defined as a nonlinear function of SOC:

$$V_{\mathrm{oc}} = \kappa_1 Z + \kappa_2 \tag{4}$$

where κ_1 and κ_2 are obtained by battery test data and are considered to be constant in some range of SOC.

The derivative of terminal voltage can be expressed on the assumption that the derivative of input current is 0 as

$$\begin{aligned}\dot{V}_{\mathrm{t}} &= \dot{V}_{\mathrm{oc}} + \dot{V}_{\mathrm{p}} \\ &= \frac{I}{C_{\mathrm{n}}} - \frac{1}{R_{\mathrm{p}}C_{\mathrm{p}}}V_{\mathrm{p}} + \frac{I}{C_{\mathrm{p}}} = -\frac{1}{R_{\mathrm{p}}C_{\mathrm{p}}}V_{\mathrm{t}} + \frac{1}{R_{\mathrm{p}}C_{\mathrm{p}}}V_{\mathrm{oc}} + \left(\frac{1}{C_{\mathrm{n}}} + \frac{1}{C_{\mathrm{p}}} + \frac{R_{\mathrm{t}}}{R_{\mathrm{p}}C_{\mathrm{p}}}\right) I \\ &= -a_1 V_{\mathrm{t}} + a_1 V_{\mathrm{oc}} + b_1 I \end{aligned} \tag{5}$$

The equation of SOC and polarization voltage can be rewritten as

$$\dot{Z} = \frac{1}{R_{\mathrm{t}}C_{\mathrm{n}}}\left(V_{\mathrm{t}} - V_{\mathrm{oc}} - V_{\mathrm{p}}\right) = a_2 V_{\mathrm{t}} - a_2 V_{\mathrm{oc}} - a_2 V_{\mathrm{p}} \tag{6}$$

$$\dot{V}_{\mathrm{p}} = -\frac{1}{R_{\mathrm{p}}C_{\mathrm{p}}}V_{\mathrm{p}} + \frac{I}{C_{\mathrm{p}}} = -a_1 V_{\mathrm{p}} + b_2 I \tag{7}$$

where $a_1 = \frac{1}{R_{\mathrm{p}}C_{\mathrm{p}}}$, $a_2 = \frac{1}{R_{\mathrm{t}}C_{\mathrm{n}}}$, $b_1 = \frac{1}{C_{\mathrm{n}}} + \frac{1}{C_{\mathrm{p}}} + \frac{R_{\mathrm{t}}}{R_{\mathrm{p}}C_{\mathrm{p}}}$, $b_2 = \frac{1}{C_{\mathrm{p}}}$.

Terminal voltage is selected as output of the system:

$$y = \begin{bmatrix} 1 & 0 & 0 \end{bmatrix} \begin{bmatrix} V_{\mathrm{t}} & Z & V_{\mathrm{p}} \end{bmatrix}^{\mathrm{T}} \tag{8}$$

Figure 2 shows a battery pack in which multiple single cells are connected in series. This paper selects the Thevenin model to model the ith cell. The terminal voltage of each cell in the series battery pack is measured by a voltage sensor, the input current of the pack is measured by a current sensor and transmitted to the BMS. Combining the state

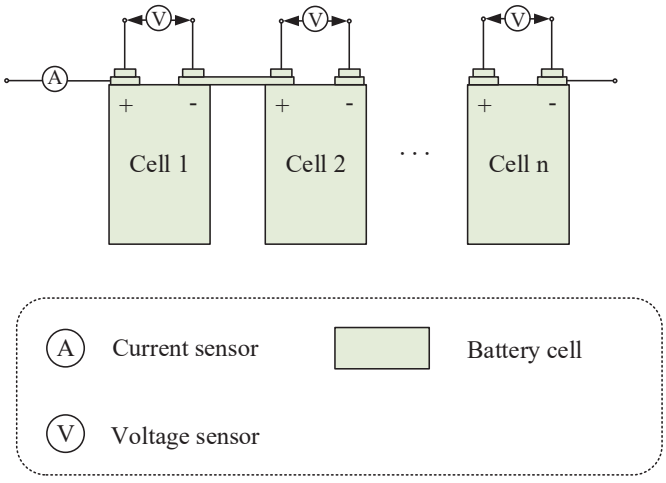

(a) Schematic diagram of battery pack used in this study

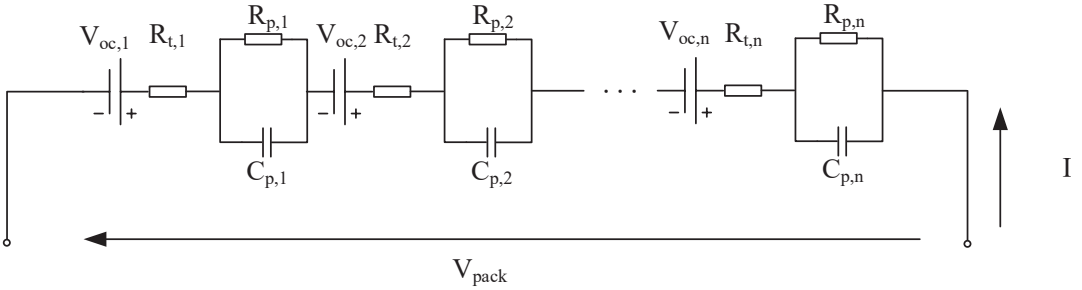

(b) ECM of a serial battery

FIGURE 2. Schematic diagram and model of a serial battery

space equation (5)-(8), mathematical representation of the battery pack can be arranged as

$$\begin{cases} \dot{x}_i = A_i x_i + B_i u_i \\ y_i = C_i x_i \end{cases} \tag{9}$$

where $x_i = \begin{bmatrix} V_{ti} & Z_i & V_{pi} \end{bmatrix}^{\mathrm{T}}$, $y_i = V_{ti}$, $A_i = \begin{bmatrix} -a_{1i} & a_{1i} & 0 \\ a_{2i} & -a_{2i} & -a_{2i} \\ 0 & 0 & -a_{1i} \end{bmatrix}$, $B_i = \begin{bmatrix} b_{1i} \\ 0 \\ b_{2i} \end{bmatrix}$, $C_i = \begin{bmatrix} 1 \\ 0 \\ 0 \end{bmatrix}$.

There are some errors between the ECM model and the real battery data. Consequently, the disturbance terms are put in the model to make up for the modeling errors. The battery model can be expressed as

$$\begin{cases} \dot{x}_i = (A_i + \Delta A_i)x_i + (B_i + \Delta B_i)u_i \\ y_i = (C_i + \Delta C_i)x_i \end{cases} \tag{10}$$

where ΔA_i, ΔB_i and ΔC_i denote the parameters of uncertainties with appropriate dimensions. Considering the uncertainties, the model can be represented as

$$\omega_i = \Delta A_i x_i + \Delta B_i u_i \tag{11}$$

$$v_i = \Delta C_i x_i \tag{12}$$

Then, the dynamic battery model can be expressed as

$$\begin{cases} \dot{x}_i = A_i x_i + B_i u_i + \omega_i \\ y_i = C_i x_i + v_i \end{cases} \tag{13}$$

Assumption 2.1. *Matrix (A_i, C_i) is observable.*

Assumption 2.2. *There exists matrix $L \in R^{n\times n}$ such that $A_{0i} = A_i - LC_i$ is a stable matrix.*

Assumption 2.3. *There exists Lyapunov equation $A_{0i}^{\mathrm{T}}P + PA_{0i} = -Q$, where P, Q are symmetric positive definite matrices.*

Assumption 2.4. *There exists matrix G such that $PB_i = C_i^{\mathrm{T}}G^{\mathrm{T}}$.*

Assumption 2.5. *ω_i is norm bounded, $\|\omega_i\| \leqslant \theta$, fault f_s is bounded, $\|f_s\| \leqslant \varphi$, where φ is positive constant and $\theta \ll \varphi$.*

3. Model-Based Fault Diagnosis Scheme.

In order to realize model-based sensor fault diagnosis, this section first introduces the model reconstruction of the battery and the SMO for fault diagnosis, and then uses the output of the SMO and the output of the system to construct the residual error that can be used to detect the fault.

The scheme of fault diagnosis based on SMO is shown in Figure 3. The signal from the mathematical model is compared with the measured signal, and the filtered difference forms a residual signal. In the case of no obstacle, the residual is zero, and in case of failure, the residual is not zero. The residual signal has a certain threshold to avoid false alarm due to uncertainty. When the residual signal exceeds the threshold, the fault will be determined. The SMO works in synchronization with the battery system, makes the state estimation of the battery according to the measured value of current and voltage, and further predicts the battery output voltage and SOC. Then, by comparing the output voltage and SOC estimated and measured by the SMO, the residual error with the fault information is generated and evaluated. In this paper, it is assumed that only one failure exists in a cell at a time.

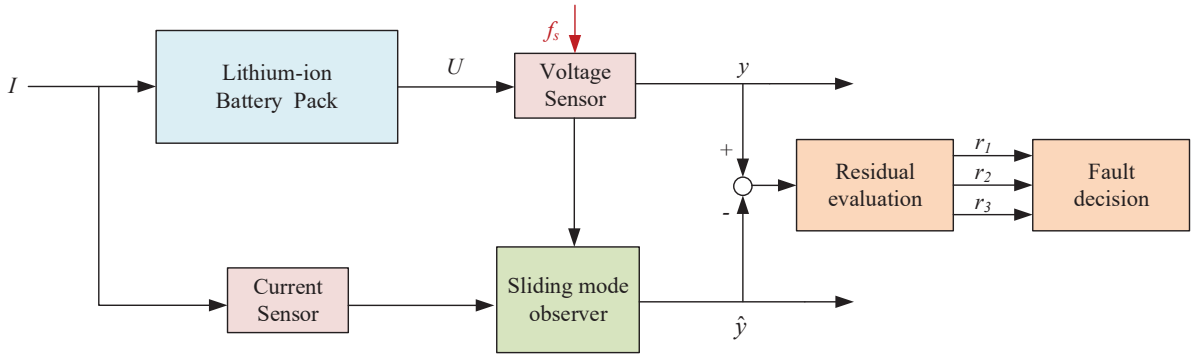

FIGURE 3. Schematic of the proposed fault diagnosis

3.1. **System under sensor faults.** Since voltage sensors are mainly Hall effect sensors, the most common types of sensor fault in battery systems are bias fault and gain fault, which can be considered as additive faults [27]. When a sensor fault occurs, the voltage output signal can be represented by using f_s to indicate sensor failure as

$$y = x + f_s \tag{14}$$

where y is the measured value of sensor, x is the system input, and f_s is the fault value.

3.2. **Design of the sliding mode observer.** When the battery system generates voltage sensor fault, the model can be rewritten as

$$\begin{cases} \dot{x}_i = A_i x_i + B_i u_i + D_i \omega_i \\ y_i = C_i x_i + F_i f_{si} \end{cases} \tag{15}$$

where f_{si} is sensor fault signal, D_i is disturbance distribution matrix, and F_i is the fault distribution matrix.

Theorem 3.1. *An additive fault can be detected if and only if* $C_i(sI - A_i)^{-1}B_i + F_{fm} \neq 0$, *where* F_{fm} *is the* m*th column vector of matrix* F_f.

Based on the condition that the fault can be detected, the SMO for battery system is designed as

$$\begin{cases} \dot{\hat{x}}_i = A_i \hat{x}_i - L(\hat{y}_i - y_i) + B_i u_i + D_i \mu_i \\ \hat{y}_i = C_i \hat{x}_i \end{cases} \tag{16}$$

where L is observer gain matrix, μ_i is the function of sliding mode control law, which is used to suppress the influence of disturbance, its expression is as follows:

$$\mu_i = -\rho \frac{G_i e_{yi}}{\|G_i e_{yi}\| + \delta} \tag{17}$$

where switching gain of SMO satisfies $\rho > \varphi$, G_i is the ith row vector of matrix G, $e_{yi} = C\hat{x}_i - y_i$, δ is a positive constant with a very small scalar, which is to ensure the continuity of nonlinear terms.

Suppose the fault occurs in group l, define state deviation $e_l = \hat{x}_l - x_l$, then output deviation $e_{yl} = \hat{y}_l - y_l = C_l e_l - F_l f_{sl}$. The state deviation equation can be expressed as

$$\dot{e}_l = A_{0l} e_l + D_l(\mu_l - \omega_l) + L F_l f_{sl} \tag{18}$$

The residual is expressed by the output deviation:

$$r_l = e_{yl} = C_l e_l - F_l f_{sl} \tag{19}$$

When there is no fault, $f_{sl} = 0$, residual $r_l = C_l e_l$, state deviation equation can be expressed as

$$\dot{e}_l = A_{0l} e_l + D_l(\mu_l - \omega_l) \tag{20}$$

The state deviation will be stable in the zero domain, so it is known from the residual expression that r_l will also be stable in the zero domain.

When there is a sensor fault, $f_{sl} \neq 0$, residual $r_l = C_l e_l - F_l f_{sl}$, state deviation equation can be expressed as Equation (18).

The residual error of this fault condition will be very sensitive, that is, the residual error will immediately deviate from the zero domain. The residual deviation from the zero domain will not be stable.

3.3. **Stability analysis.** Select Lyapunov function as

$$V = e_i^{\mathrm{T}} P e_i \tag{21}$$

where V is positive definite. Taking the derivative of Lyapunov function, one has

$$\begin{aligned}
\dot{V} &= \dot{e}_i^{\mathrm{T}} P e_i + e_i^{\mathrm{T}} P \dot{e}_i \\
&= e_i^{\mathrm{T}} \left(P A_{0i} + A_{0i}^{\mathrm{T}} P \right) e_i + 2 e_i^{\mathrm{T}} P D_i (\mu_i - \omega_i) \\
&= -e_i^{\mathrm{T}} Q e_i + 2 (G_i C_i e)^{\mathrm{T}} (\mu_i - \omega_i) \\
&\leqslant - \parallel Q \parallel \cdot \parallel e_i \parallel^2 - 2\rho \parallel G_i e_{yi} \parallel + 2 \parallel G_i e_{yi} \parallel \cdot \parallel \omega_i \parallel \\
&\leqslant -2 \parallel G_i e_{yi} \parallel (\rho - \parallel \omega_i \parallel) \\
&\leqslant 0
\end{aligned} \tag{22}$$

Therefore, according to Lyapunov stability principle, e_i will be stable near the zero domain.

3.4. **Residual evaluation.** By reason of existing modeling error and measurement noise, the residual error is ever present even in case of no system failure. In order to reduce false alarms, the residual between the estimated value and the actual value is compared with the threshold value to determine whether there is a fault. CUSUM is a frequently used statistical technique that can effectively detect sudden changes [29,30]. The statistical signal is defined as

$$s_k = \left(\frac{\bar{\mu}_f - \bar{\mu}_n}{\sigma_n^2} \right) \times \left(\hat{r} - \frac{\bar{\mu}_f + \bar{\mu}_n}{2} \right) \tag{23}$$

where $\bar{\mu}_f$, $\bar{\mu}_n$ are mean values under fault condition and normal condition, σ_n^2 is standard deviation value under normal condition, and $\hat{r}$ is the considered measure for the kth observation.

The cumulative sum is defined as

$$S(k) = \sum_{k=1}^{N} s_k \tag{24}$$

where N means number of samples.

The decision law and fault flag are identified as

$$D_{S_k} = S(k) - S(k)_{\min} \tag{25}$$

$$Flag = \begin{cases} 1, & D_{S_k} > J, \quad f_s \neq 0 \\ 0, & D_{S_k} < J, \quad f_s = 0 \end{cases} \tag{26}$$

where J is the designed threshold.

4. Faults Effects Analysis.

4.1. Parameter setting.

The proposed scheme is designed and its stability is proved in Section 3. The purpose of this section is to verify the effectiveness and robustness of the proposed scheme via simulation. Experiments have been conducted by Arbin BT2000 battery charging and discharging test system and ESPEC PRA-3AP temperature and humidity chamber. Numerical simulation will be given based on INR 18650-20R LIB cell. Its performance parameters are shown in Table 1 [28].

Table 1. Performance parameters of INR 18650-20R LIB cell

Nominal capacity	2000 mAh
Nominal voltage	3.6 V
Upper cut-off voltage	4.20 ± 0.05 V
Lower cut-off voltage	2.50 ± 0.05 V
Standard charging	CCCV, 1 A, 100 mA cut-off
Standard discharging	CCCV, 4 A, 100 mA cut-off
Charging time	180 min/100 mA cut-off
Maximum discharge current	22 A (at 25°C)
Charging temperature	$0 \sim 50$°C
Discharging temperature	$-20 \sim 75$°C

The research object of this paper is a series power battery composed of three INR 18650-20R LIB cells in series. The dynamic stress test (DST) is performed for 80% battery level at 25°C, the sampling time for each time point is 1 s. Figure 4(a) plots the input current. Figure 4(b) plots the input current during discharge period. Figure 4(c) plots the battery test loading profiles under DST test. Figure 4(d) plots the experimental output voltage of a single cell. Figure 4(e) plots the experimental monomer voltage of three batteries. Figure 4(f) plots the series battery voltage. This paper chooses the current profile in the discharge period under DST test as the input. The simulation time is set to 10000 s.

Battery ECM parameter identification results are obtained by recursive least squares with forgetting factor (FFRLS) method and curve fitting toolbox, the forgetting factor is usually selected between 0.95-1. In this paper, 0.97 is selected as the appropriate forgetting factor owing to the good convergence results. The identification results are shown in Figure 5; fitted parameter identification results of equivalent circuit model are summarized in Table 2.

4.2. Simulation analysis.

Voltage sensor faults with different time and size are simulated and verified. A voltage sensor fault of 0.1 V deviation is injected into the voltage sensor of cell 1# at 5000 s and another voltage sensor fault of 0.15 V deviation is injected into the voltage sensor of cell 2# at 5000 s.

It can be seen from Figure 6 that the estimated values of SOC1 and SOC2 deviate from the true value after 5000 s by degrees respectively. It can be inferred from the simulation results that voltage sensor faults will have negative effects on the battery SOC estimations and may cause problems with BMS. When the voltage sensor has additional faults, the SOC estimated by the sliding mode observer is about 15.6% and 21.5% at 10000 s. In order to protect the battery and prevent overcharge and over-discharge, BMS will issue a command to stop discharging when the SOC of the battery is lower than a certain value. However, in the case of voltage sensor failure, the estimation of SOC will deviate. BMS will give instructions for the battery to continue to discharge when the SOC is lower

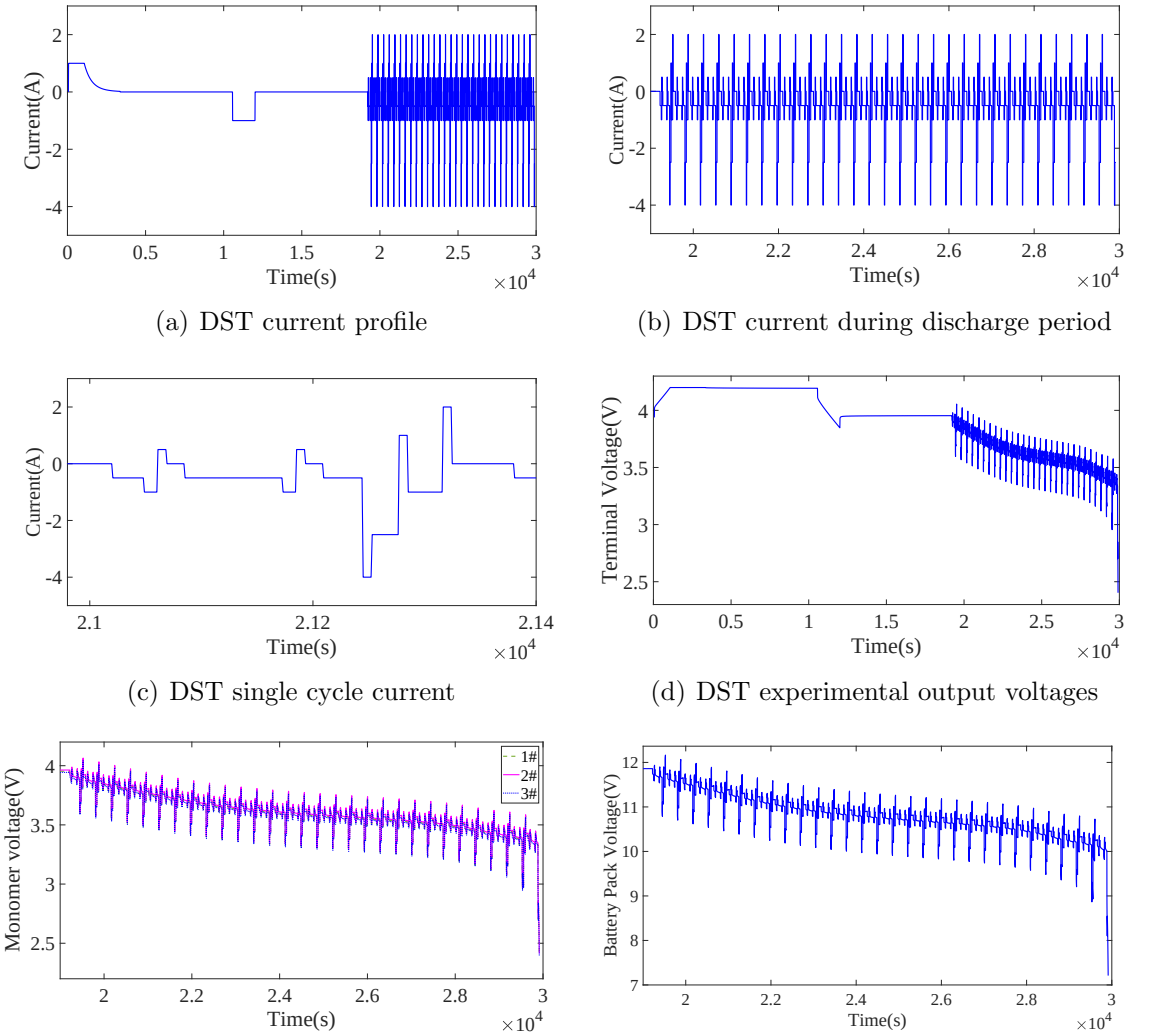

(a) DST current profile

(b) DST current during discharge period

(c) DST single cycle current

(d) DST experimental output voltages

(e) Monomer voltage during discharge period

(f) Battery pack voltage during discharge period

FIGURE 4. Current and voltage under DST test

than the cut-off SOC, the battery will remain in the low SOC state, which will lead to over-discharge of the battery, accelerate the aging of the battery and result in shortening the span of battery life.

Figure 7 shows the comparison of SOC estimation errors in different health states. The RMSEs of SOC estimation are 0.081, 0.118 and 0.026, respectively. The numerical indexes of cell 1# and cell 2# are higher than that of the normal cell. In addition, the larger size of the deviation signal, the greater SOC estimation error.

It can be seen from Figure 8 that the residuals of cell 1# and cell 2# grow evidently after the occurrence of sensor fault. It can be seen from Figure 9 that the residual of cell 3# remains in a small range all the time while the residuals of cell 1# and cell 2# exceed the safe range after 5000 s. The residual of cell 1# continues to grow and exceeds the set threshold at 5029 s while the residual of cell 2# exceeds the set threshold at 5017 s. The validation results show the effectiveness of the SMO diagnosis scheme. Furthermore, residual error is proved to make no difference on fault diagnosis result.

Consider injecting aforementioned faults of the same size into the sensor of cells at different times. A fault of 0.1 V deviation is injected into the voltage sensor of cell 1# at 5500 s and another fault of 0.15 V deviation is injected into the voltage sensor of cell

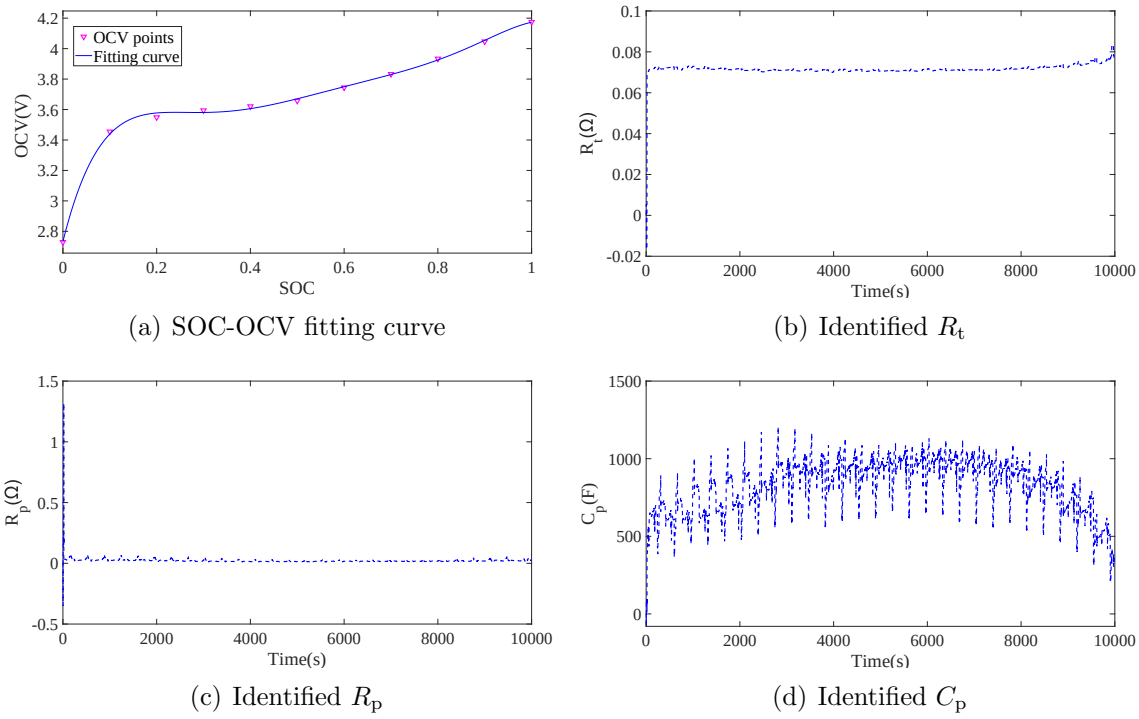

(a) SOC-OCV fitting curve (b) Identified R_{t}

(c) Identified R_{p} (d) Identified C_{p}

FIGURE 5. Parameters identification results

TABLE 2. Parameters of INR 18650-20R LIB cell

R_{t}	0.0701 Ω
R_{p}	0.0269 Ω
C_{p}	808 F
C_{n}	2000 mAh
$V_{\mathrm{oc}}(Z)$	$0.839Z + 3.273$

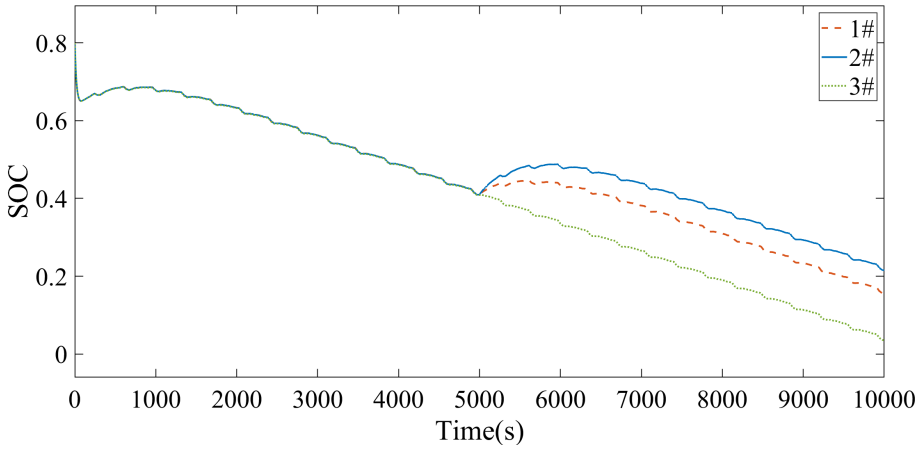

FIGURE 6. Comparison of SOC estimation results in different health states

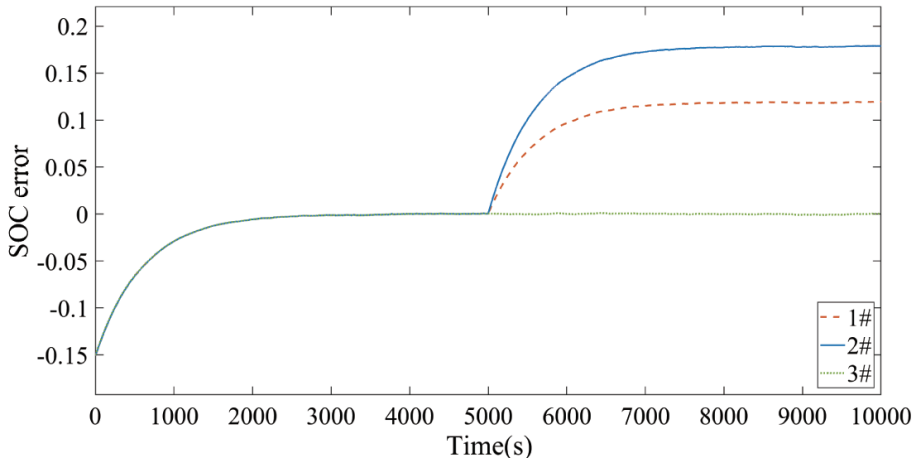

FIGURE 7. Comparison of SOC estimation errors in different health states

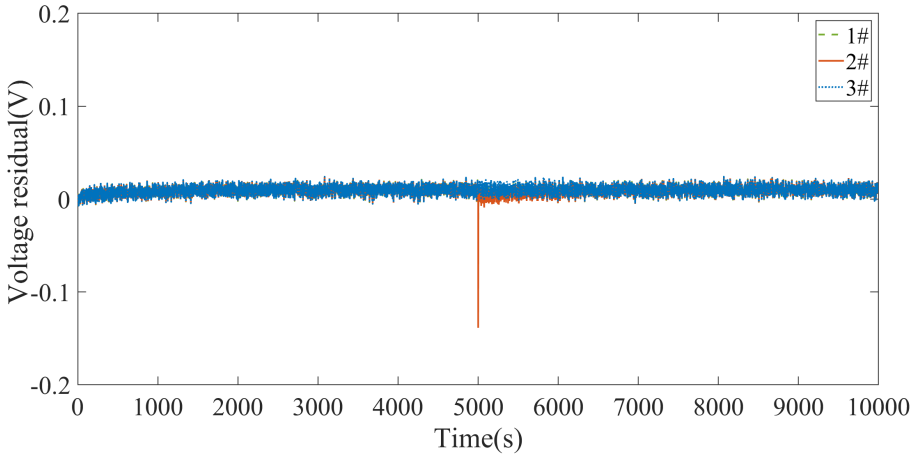

FIGURE 8. Profiles of voltage residuals with injection time at 5000 s

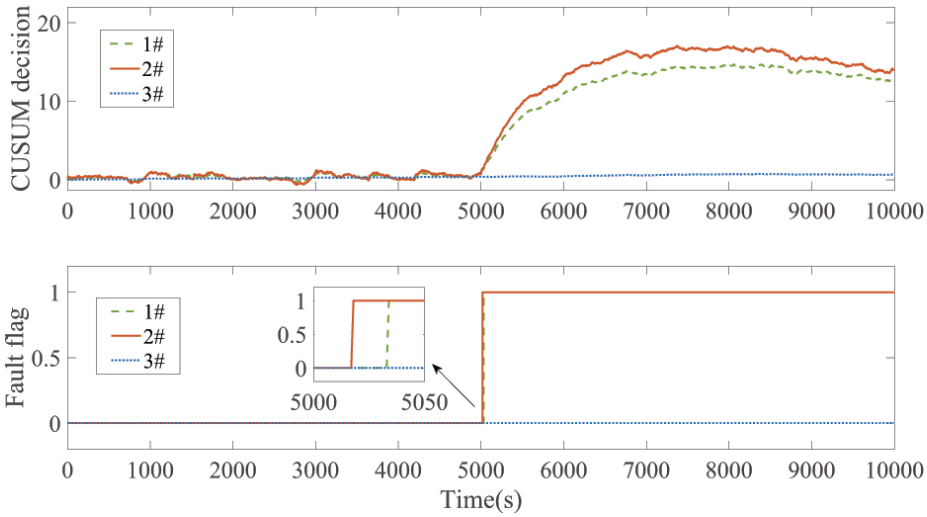

FIGURE 9. Fault detection with injection time at 5000 s

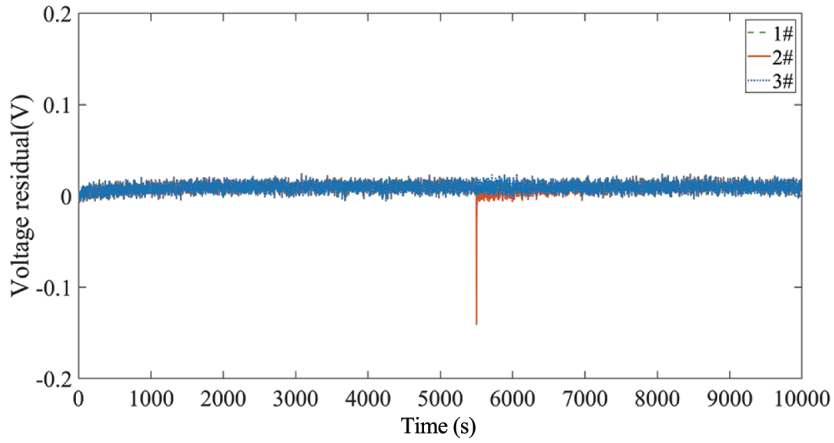

FIGURE 10. Profiles of voltage residuals with injection time at 5500 s

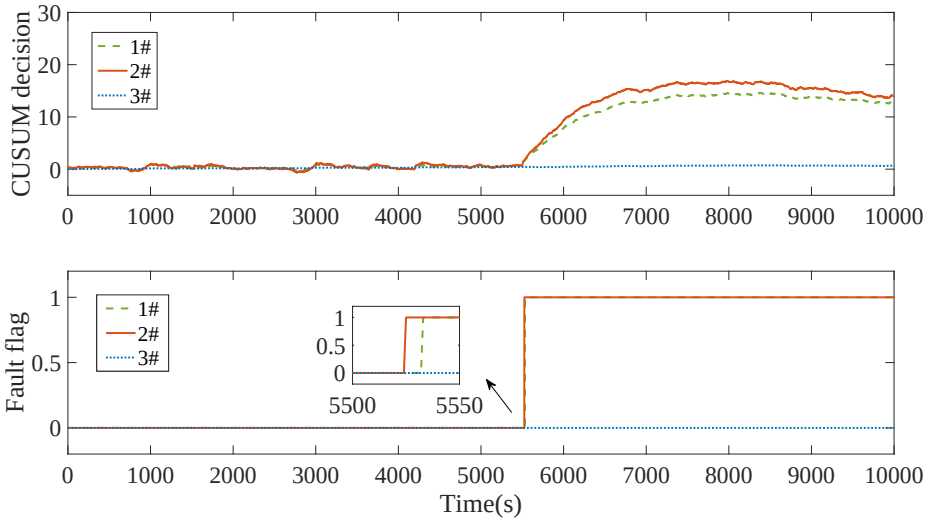

FIGURE 11. Fault detection with injection time at 5500 s

2# at 5500 s. Figure 10 shows voltage residuals with injection time at 5500 s. It can be seen from Figure 11 that it takes 36 s to detect the fault of the voltage sensor of cell 1# while it takes 22 s to detect the fault of the voltage sensor of cell 2#. It can be inferred from detection time that the larger and earlier the deviation is injected into the voltage sensor, the shorter it will take to realize fault diagnosis.

Figure 12 and Figure 13 show the results of battery fault diagnosis based on Kalman filter method. As can be seen from the figures, compared with SMO method, the residuals are larger, the time required to detect the occurrence of the fault is longer, the response speed is slower, and the detection accuracy is lower.

The experimental results show that the established system model can well describe the electrical dynamic behavior characteristics of the battery pack, and the proposed FD scheme can detect sensor faults accurately, reliably and quickly.

5. **Conclusions.** A model-based sensor fault diagnosis method is proposed in this paper. Based on Thevenin equivalent circuit model, a sliding mode observer is designed for the system, and the output deviation of the observer is taken as the residual signal. It is theoretically analyzed that the residual is only sensitive to the fault, but not to the disturbance. Then, in order to detect the system fault more accurately and reduce the

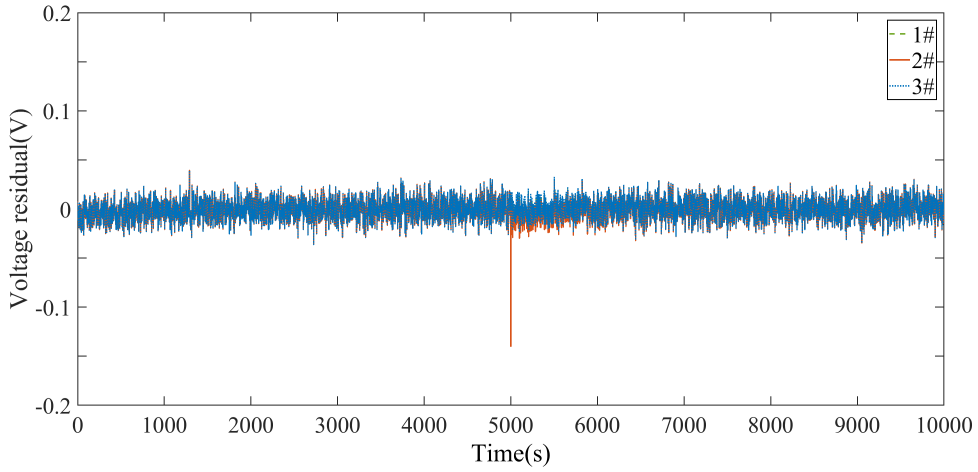

FIGURE 12. Profiles of voltage residuals

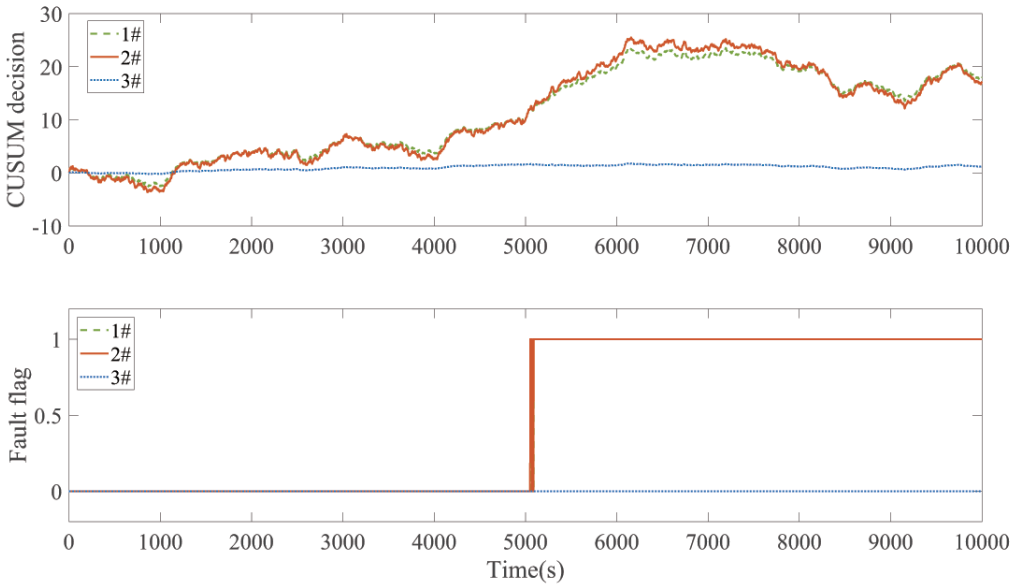

FIGURE 13. Fault detection

misdiagnosis rate, the residual error is compared with the threshold value to determine whether the system has a fault. Finally, the proposed fault detection method is verified to be effective and robust by the simulation of the battery system.

However, some limitations of this work still remain. For example, the case of multiple failures of the battery system is not considered, and only the case of simultaneous sensor failures is considered. In the future research, the impact of multi-type sensor failures on the battery system must be considered.

Acknowledgment. This work is partially supported by the National Natural Science Foundation of China (62222307, 61973140), and the Natural Science Foundation of Jiangsu Province (BK20211235). The authors also gratefully acknowledge the helpful comments and suggestions of the reviewers, which have improved the presentation.

REFERENCES

[1] B. Scrosati and J. Garche, Lithium batteries: Status, prospects and future, *Journal of Power Sources*, vol.195, no.9, pp.2419-2430, 2010.

[2] Q. Liu, D. Xu, B. Jiang and Y. Ren, Prescribed-performance-based adaptive control for hybrid energy storage systems of battery and supercapacitor in electric vehicles, *International Journal of Innovative Computing, Information and Control*, vol.16, no.2, pp.571-583, 2020.
[3] L. Lu, X. Han, J. Li et al., A review on the key issues for lithium-ion battery management in electric vehicles, *Journal of Power Sources*, vol.226, pp.272-288, 2013.
[4] X. Han, H. He, L. Hu et al., Energy management based on reinforcement learning with double deep Q-learning for a hybrid electric tracked vehicle, *Applied Energy*, vol.254, 113708, 2019.
[5] F. Feng, X. Hu, L. Hu et al., Propagation mechanisms and diagnosis of parameter inconsistency within Li-Ion battery packs, *Renewable and Sustainable Energy Reviews*, vol.112, pp.102-113, 2019.
[6] L. Yao, Z. Wang and J. Ma, Fault detection of the connection of lithium-ion power batteries based on entropy for electric vehicles, *Journal of Power Sources*, vol.293, pp.548-561, 2015.
[7] Z. A. Biron, P. Pisu and B. Ayalew, Observer-based diagnostic scheme for lithium-ion batteries, *Dynamic Systems and Control Conference*, 2015.
[8] S. Dey, Z. Biron, S. Tatipamula et al., Model-based real-time thermal fault diagnosis of lithium-ion batteries, *Control Engineering Practice*, vol.56, pp.37-48, 2016.
[9] X. Li and Z. Wang, A novel fault diagnosis method for lithium-ion battery packs of electric vehicles, *Measurement*, vol.116, pp.402-411, 2018.
[10] R. Xiong, Q. Yu, W. Shen et al., A sensor fault diagnosis method for a lithium-ion battery pack in electric vehicles, *IEEE Transactions on Power Electronics*, vol.34, no.10, pp.9709-9718, 2019.
[11] Z. Liu and H. He, Model-based sensor fault diagnosis of a lithium-ion battery in electric vehicles, *Energies*, vol.8, pp.6509-6527, 2015.
[12] Z. Chen, K. Xu, J. Wei et al., Voltage fault detection for lithium-ion battery pack using local outlier factor, *Measurement*, vol.146, pp.544-556, 2019.
[13] Y. Shang, G. Lu, Y. Kang et al., A multi-fault diagnosis method based on modified sample entropy for lithium-ion battery strings, *Journal of Power Sources*, vol.446, no.15, 227275, 2020.
[14] X. Wang, S. Wang, S. An and H. Liu, An adaptive disturbance suppression based fault-tolerant control approach against the control surface faults, *International Journal of Innovative Computing, Information and Control*, vol.19, no.1, pp.213-227, 2023.
[15] Z. Liu and H. He, Sensor fault detection and isolation for a lithium-ion battery pack in electric vehicles using adaptive extended Kalman filter, *Applied Energy*, vol.185, pp.2033-2044, 2016.
[16] C. Zheng, Z. Chen and D. Huang, Fault diagnosis of voltage sensor and current sensor for lithium-ion battery pack using hybrid system modeling and unscented particle filter, *Energy*, vol.191, no.2, 116504, 2020.
[17] J. Wei, G. Dong and Z. Chen, Lyapunov-based thermal fault diagnosis of cylindrical lithium-ion batteries, *IEEE Transactions on Industrial Electronics*, vol.67, no.6, pp.4670-4679, 2019.
[18] J. Tian, Y. Wang and Z. Chen, Sensor fault diagnosis for lithium-ion battery packs based on thermal and electrical models, *International Journal of Electrical Power & Energy Systems*, vol.121, 106087, 2020.
[19] K. Zhang, B. Jiang, X.-G. Yan and J. Xia, Distributed fault diagnosis of multi-agent systems with time-varying sensor faults, *ICIC Express Letters*, vol.14, no.2, pp.129-135, 2020.
[20] C. Edwards, S. K. Spurgeon and R. J. Patton, Sliding mode observers for fault detection and isolation, *Automatica*, vol.36, no.4, pp.541-553, 2000.
[21] C. P. Tan and C. Edwards, Sliding mode observers for detection and reconstruction of sensor faults, *Automatica*, vol.38, no.10, pp.1815-1821, 2002.
[22] C. P. Tan and C. Edwards, Sliding mode observers for robust detection and reconstruction of actuator and sensor faults, *International Journal of Robust and Nonlinear Control: IFAC-Affiliated Journal*, vol.13, no.5, pp.443-463, 2003.
[23] X. G. Yan and C. Edwards, Sensor fault detection and isolation for nonlinear systems based on a sliding mode observer, *International Journal of Adaptive Control and Signal Processing*, vol.21, nos.8-9, pp.657-673, 2007.
[24] F. J. J. Hermans and M. B. Zarrop, Sliding mode observers for robust sensor monitoring, *IFAC Proceedings Volumes*, vol.29, no.1, pp.6530-6535, 1996.
[25] S. Dey, S. Mohon, P. Pisu et al., Sensor fault detection, isolation, and estimation in lithium-ion batteries, *IEEE Transactions on Control Systems Technology*, vol.24, no.6, pp.2141-2149, 2016.
[26] J. Sun, Y. Qiu, Y. Shang et al., A multi-fault advanced diagnosis method based on sparse data observers for lithium-ion batteries, *Journal of Energy Storage*, vol.50, 104694, 2022.
[27] E. Balaban, A. Saxena, P. Bansal et al., Modeling, detection, and disambiguation of sensor faults for aerospace applications, *IEEE Sensors Journal*, vol.9, no.12, pp.1907-1917, 2009.

[28] *https://web.calce.umd.edu/batteries/data.htm*, 2015.
[29] J. Meng, M. Boukhnifer, C. Delpha et al., Incipient short-circuit fault diagnosis of lithium-ion batteries, *Journal of Energy Storage*, vol.31, 101658, 2020.
[30] C. Delpha, D. Diallo, H. Al Samrout et al., Multiple incipient fault diagnosis in three-phase electrical systems using multivariate statistical signal processing, *Engineering Applications of Artificial Intelligence*, vol.73, pp.68-79, 2018.

Author Biography

Dezhi Xu received the Ph.D. degree in Control Theory and Control Engineering from Nanjing University of Aeronautics and Astronautics, China, in 2013.

He was a Visiting Fellow with the Department of Biomedical Engineering, City University of Hong Kong, Hong Kong, from 2018 to 2019. He is currently a Professor and Doctoral Supervisor with the Jiangnan University. His current research interests include data driven-control, fault diagnosis and fault-tolerant control, multi-agent systems and CPSs, technologies of renewable energy, motor control, and smart grid. Prof. Xu was a recipient of the First Class Prize of Science and Technology Progression from the China General Chamber of Commerce in 2016, and the Best Young Scholar of Jiangnan University in 2022 for his research results. He is currently a Guest Editor or an Editorial Board Member for a number of journals, such as the *International Journal of Innovative Computing, Information and Control*, the *Electric Power*, the *Zhejiang Electric Power*, the *Electrotechnical Application*, and the *Electrical Engineering*. He is a Committee Member of the Association of Energy Internet, and Trusted Control in Chinese Association of Automation (CAA), and the Energy Storage in China Renewable Energy Society (CRES).

Yunchen Ma received the B.S. degree in Electrical Engineering and Automation from Southwest Jiaotong University in Chengdu, China, in 2019. She is currently pursuing the M.S. degree in electrical engineering with Jiangnan University, Wuxi, China.

Her current research interests include fault diagnosis of battery system.

Weilin Yang received his B.Eng. degree in Machine Design & Manufacture and Their Automation from University of Science and Technology of China, Hefei, China, in 2009, and the Ph.D. degree in Mechanical Engineering from City University of Hong Kong, Hong Kong SAR in 2013.

He was a postdoctoral researcher at Masdar Institute of Science and Technology (now Khalifa University), Abu Dhabi, UAE, 2013-2016. He was a research engineer of General Electric (GE) Global Research, Shanghai, 2016-2017. He joined Jiangnan University in July 2017, where he is currently an Associate Professor. His research interests include modeling and control of energy systems, robust model predictive control, and dada-driven control.

Tinglong Pan received his B.Eng. degree in Industrial Automation from China University of Mining and Technology, Xuzhou, China, in 1999, and the Ph.D. degree in Power Electronics and Power Drive from China University of Mining and Technology, Xuzhou, China, in 2004.

He is currently a Professor at Jiangnan University, where his research interests include microgrid control technology, power conversion technology, power drive system and its intelligent control technology.

Zhenlan Dou received the Ph.D. degree in Motors and Electrical Appliances from Shanghai Jiao Tong University, China, in 2013.

She has long been engaged in wind power generation, energy storage, micro grid, distributed energy, integrated energy system and its control technology research and engineering application demonstration. Ms. Zhenlan Dou, a senior engineer, is currently the Technical Director of Integrated Energy Company of State Grid Shanghai Municipal Electric Power Company.